IEEE Access
Multidisciplinary | Rapid Review | Open Access Journal

Received November 18, 2019, accepted November 28, 2019, date of publication December 2, 2019,
date of current version December 13, 2019.

Digital Object Identifier 10.1109/ACCESS.2019.2957046

Design and Analysis of a 4-kW Two-Stack Coreless Axial Flux Permanent Magnet Synchronous Machine for Low-Speed Applications

SAHIB KHAN[1], SYED SABIR HUSSAIN BUKHARI[1,2], (Member, IEEE), AND JONG-SUK RO[2], (Member, IEEE)

[1]Department of Electrical Engineering, Sukkur IBA University, Sukkur 65200, Pakistan
[2]School of Electrical and Electronics Engineering, Chung-Ang University, Seoul 06974, South Korea

Corresponding author: Jong-Suk Ro (jongsukro@gmail.com)

This work was supported in part by the National Research Foundation of Korea funded by the Ministry of Education under Grant 2016R1D1A1B01008058, in part by the Korea Electric Power Corporation under Grant R17XA05-30, and in part by the Korea Research Fellowship Program through the National Research Foundation (NRF) of Korea funded by the Ministry of Science and ICT under Grant 2019H1D3A1A01102988.

ABSTRACT This paper presents a comparative performance analysis of 4-kW axial flux permanent magnet synchronous machines (AFPMSMs) with and without a rotor core. The present study is intended for low-speed applications; however, the investigated machines are designed using an improved diameter-to-length method and their comparative performance is assessed using comprehensive electromagnetic finite element analysis. The results of this analysis suggest that the proposed coreless topology has the advantages of higher output power, higher efficiency, and lower iron or core losses compared to the conventional iron core AFPMSM.

INDEX TERMS Axial flux, coreless stator, low-speed applications, permanent-magnet, synchronous machines.

I. INTRODUCTION

Synchronous machines can be built using a wound rotor structure or a permanent magnet (PM) rotor [1]. Permanent-magnet synchronous machines (PMSMs) tend to be favored over wound rotor synchronous machines (WRSMs) [2] for low-speed applications. PM machines are more efficient than their field-excited counterparts [3], [4] because the rotor field is generated by permanent magnets mounted on the rotor surface rather than a brushed or brushless field excitation circuit [5], [6]. This increases their reliability and reduces their maintenance costs [7], [8].

Permanent magnet synchronous machines (PMSMs) are generally classified into three categories based on the direction of the flux flow: a) radial, b) axial, and c) transverse flux [9]–[11]. In addition to the conventional advantages associated with PM machines, axial flux permanent magnet (AFPM) machines have distinct advantages compared to their counterparts [10], [12]–[15] including a high torque-to-weight ratio, higher power density, higher efficiency, and a more compact structure [16], [17]. These positive features have encouraged researchers to develop new applications for AFPM machines and to make them more compatible with the modern power market [18]. Major applications of AFPM machines include wind power systems, wheel motors, hybrid vehicles, and robotics [19]–[22].

This paper proposes a high-efficiency 4-kW two-stack coreless axial flux permanent magnet (AFPM) machine for low-speed applications such as wind power generating systems, etc. First, a conventional AFPM machine model with two stators and a three-rotor configuration is designed using an improved diameter-to-length (D^2L) method [23]–[25]. An AFPM machine model with an outer rotor structure similar to the conventional machine [26] but with a coreless inner-rotor structure is then developed with the goal to increase efficiency and reduce core losses. In this design, the core of the inner rotor is replaced by a thin aluminum or plastic sheet to provide mechanical support for

The associate editor coordinating the review of this manuscript and approving it for publication was Xiaodong Sun.

the permanent magnets [27]. As the proposed topology is intended for low-speed applications, it minimizes the chance for the rotor magnets to fly apart. Comparative performance analysis is carried out for the conventional and proposed AFPM machines using comprehensive electromagnetic finite element analysis (FEA) [28].

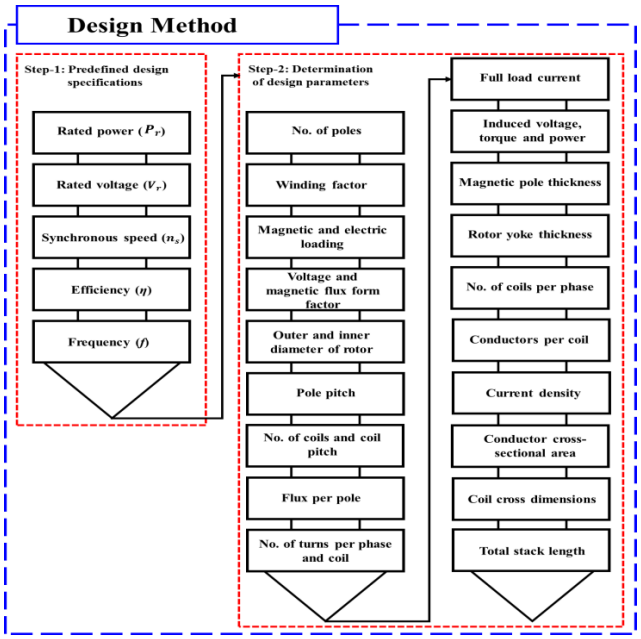

FIGURE 1. Design process for the conventional and proposed AFPM machines.

II. DESIGN METHOD FOR THE CONVENTIONAL AND PROPOSED AFPMSMs

The conventional and proposed AFPM machine models are designed using the improved D^2L design process presented in Figure 1 [23]. This design method consists of two steps which are discussed as follow:

Step 1 Predefined Design Specifications:

The design method employed for the conventional and proposed AFPM machines for low-speed applications is based on certain predefined parameters, including the rated power and voltage, operating frequency, synchronous speed, and expected efficiency of the machines. The values for these parameters are listed in Table 1.

Step 2 Determination of the Design Parameters:

The step 2 elucidates the procedure of calculation of different designing parameters for the axial flux permanent magnet synchronous machines based on the predefined design specifications using mathematical equations. Because AFPM machines have a large air gap and a disclosed PM pole structure, magnetic flux leakage and fringing may have a considerable effect on the design results. To account for these potential issues, a magnetic flux form factor is utilized in the improved design process, as shown in Figure 1. The magnetic flux form factor ε is calculated using equation (1):

$$\varepsilon = \frac{4}{\pi}\sin\left(\frac{B_{mg}}{B_r}\cdot\frac{\pi}{2}\right), \tag{1}$$

where B_{mg} and B_r are the magnetic flux and residual flux densities, respectively.

TABLE 1. Initial values for the design of conventional and proposed AFPM machines.

Parameter	Value	Unit
Rated Power	4,000	W
Rated Voltage	180	V_{rms}
Synchronous Speed	375	RPM
Frequency	50	Hz
Efficiency	90	%

The number of magnet poles is determined using equation (2) [29]–[31]:

$$p = \frac{60f}{n_s}, \tag{2}$$

where p is the number of poles, f is the supply frequency, and n_s is the synchronous speed.

The voltage form factor (σ_f) is calculated using equation (3) [23]:

$$\sigma_f = \frac{E_f}{V} \tag{3}$$

where E_f is the back EMF and V is the phase voltage.

The winding factor of the machines (K_{w1}) is determined using equation (4) [32], [33]:

$$K_{W1} = K_d k_p, \tag{4}$$

where K_d and k_p are the distribution and pitch factors, respectively.

The outer diameter of the rotor D_o is calculated using equation (5) [34], [35]:

$$D_o = \sqrt[3]{(\sigma_f \varepsilon p_r)/(\pi^2 K_D B_{mg} A_m K_{w1} n_s \eta)} \tag{5}$$

where p_r is the rated power in kW, K_D is the machine-sizing constant, A_m is the electrical loading, K_{w1} is the winding factor, and η represents the efficiency of the machines.

The machine-sizing constant is determined using equation (6), where λ is the ratio of the inner and outer diameters of the rotor, which can be taken as 0.67 [10]:

$$K_D = \frac{\left[(1+\lambda)\left(1-\lambda^2\right)\right]}{8} \tag{6}$$

The inner diameter of rotor D_i is determined using the following equation [36]:

$$D_i = \lambda D_o \tag{7}$$

The inner pole pitch τ_i is calculated using equation (8), while the outer pole pitch τ_o is calculated using equation (9) [23].

$$\tau_i = \frac{\pi D_i}{2p} \tag{8}$$

$$\tau_o = \frac{\pi D_o}{2p} \tag{9}$$

Similarly, the inner stator coil pitch ζ_i and the outer stator coil pitch ζ_o are calculated using equations (10) and (11), respectively [23]:

$$\zeta_i = \frac{\pi D_i}{s} \tag{10}$$

$$\zeta_o = \frac{\pi D_o}{s} \tag{11}$$

The total axial length (L) of the machine is calculated using equation (12) [37].

$$L = 2j(h_M + g + h_Y) + h_c \tag{12}$$

where j is the number of stacks, h_M is the magnet pole thickness, g is the air gap, h_Y is the rotor yoke thickness, and h_c is the stator coil thickness [23].

A. DESIGN OF THE CONVENTIONAL AFPM MACHINE

In the available literature, various designs of axial flux permanent magnet machines are presented. In [36] a two-stack AFPMSM with coreless stators was proposed and the performance of the machine was verified through different parameters such like voltage, output power etc. This paper proposes a two-stack axial flux machine with a coreless stator and coreless inner rotor having geometrical parameters, calculated using D^2L method and sizing equations.

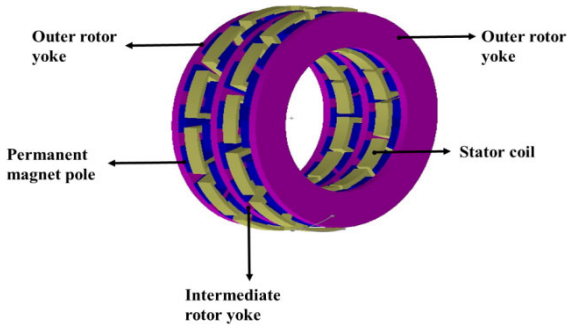

FIGURE 2. Model of the conventional AFPM machine.

The conventional AFPM machine consists of two coreless stators and three surface-mounted permanent magnet (SPM) iron-core rotors (Figure 2) [38], [39]. The output power rating of the machine is 4 kW with a rated speed of 375 rpm, and the machine operates at a supply frequency of 50 Hz. The power rating of each stack is 2 kW. The machine's design parameters are calculated using the improved D^2L process, which results in 16 rotor magnetic poles and 12 stator coils [23]. Table 2 lists the design parameters.

B. DESIGN OF THE PROPOSED AFPM MACHINE

The proposed AFPM machine presented in Figure 3 consists of two coreless stators and three rotors. The outer rotors of the proposed machine have the same configuration as the conventional AFPM machine. However, the inner rotor has a coreless structure that offers higher efficiency and reduced core losses. The core of the inner rotor in the proposed

TABLE 2. Design parameters for the conventional AFPM machine for low-speed applications.

Parameter	Value	Unit
Outer rotor diameter	346.04	mm
Inner rotor diameter	231.8	mm
Outer stator diameter	360	mm
Inner stator diameter	216	mm
Rotor yoke thickness	6.6	mm
Magnet pole thickness	8	mm
Stator coil thickness	19.5	mm
Air gap	1.5	mm
Stack length of single stack	48.4	mm
No. of stacks	2	--
Total stack length	96.8	mm
Poles per rotor disc	16	--
No. of stator coils	12	--
Outer pole pitch	67.9	mm
Turns per phase	180	--
Inner pole pitch	45.5	mm

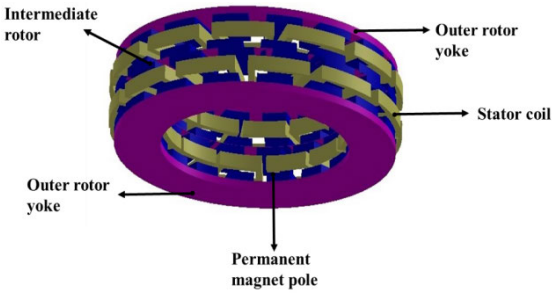

FIGURE 3. Model of the proposed AFPM machine.

machine is replaced by a thin aluminum or plastic sheet to provide mechanical support for the permanent magnets. To enable accurate comparative performance analysis of the proposed and conventional AFPM topologies, the magnetic poles are surface mounted as in the conventional topology and the rated output power, speed, and supply frequency are also identical for the two designs.

The design parameters for each stack are calculated using the improved D^2L process, which results in 16 magnetic poles for the rotor and 12 stator coils. Although the construction of the stators and outer rotors is the same for the conventional and proposed AFPM machines, the construction of the inner rotor and the stack length of the proposed AFPM machine differ from the conventional topology. Table 3 summarizes the design parameters.

III. RESULTS AND DISCUSSION

The results for the conventional and proposed AFPM machine models are obtained using finite element analysis (FEA) [40]–[42], with JMAG Designer 16.1 employed to simulate the models.

A. RESULTS FOR THE CONVENTIONAL AFPM MACHINE

The simulation results for the conventional AFPM machine are discussed in relation to the back EMF, generated output power, iron losses, and coil flux linkage. Figure 4 illustrates

TABLE 3. Design Parameters for the Proposed AFPM Machine for low-speed applications.

Parameter	Value	Unit
Outer rotor diameter	346.04	mm
Inner rotor diameter	231.8	mm
Outer stator diameter	360	mm
Inner stator diameter	216	mm
Rotor yoke thickness	6.6	mm
Magnet pole thickness	8	mm
Stator coil thickness	19.5	mm
Air gap	1.5	mm
Stack length of single stack	48.4	mm
No. of stacks	2	--
Total stack length	96.8	mm
Poles per rotor disc	16	--
No. of stator coils	12	--
Outer pole pitch	67.9	mm
Turns per phase	180	--
Inner pole pitch	45.5	mm

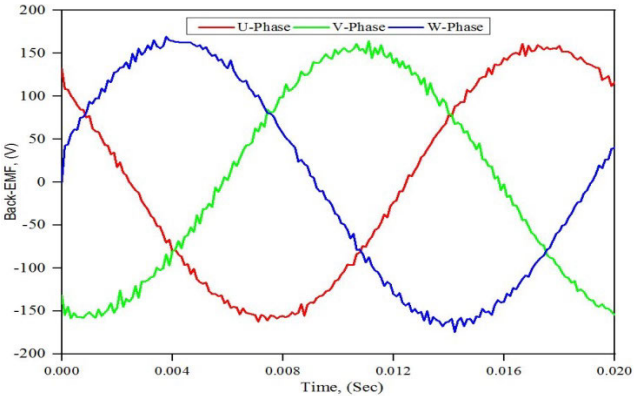

FIGURE 4. Back EMF for the conventional AFPM model.

the back EMF for the conventional model. These results are obtained through the 3-D FEA analysis under the no-load conditions. On the basis of these simulation results, the RMS value for the generated back EMF is obtained around 108.77 V. Figure 5 displays the generated output power. The average and RMS power values for this model are approximately 3,989.25 and 3,992.35 W, respectively. Figure 6 shows the iron losses generated for the conventional AFPM machine. These losses are obtained through the simulations and are calculated through the 3-D FEA analysis. The average and RMS values of the iron losses of the conventional AFPM machine are 69.33 and 74.14 W, respectively. Figure 7 displays a contour plot of the magnetic flux density for the conventional AFPM topology discussed in this paper. The FEA analysis calculates the magnetic flux density of model in order to predict the minimum and maximum flux density on the machine through its contour plot.

B. RESULTS FOR THE PROPOSED AFPM MACHINE

Figure 8 illustrates the back EMF of the proposed topology. The back EMF for the U, V, and W phases of the stator

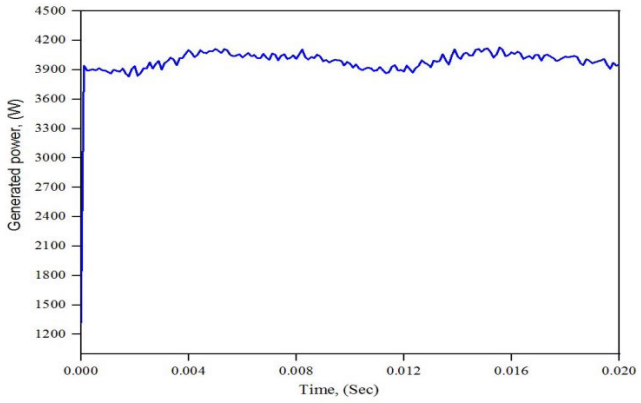

FIGURE 5. Generated output power for the conventional AFPM machine.

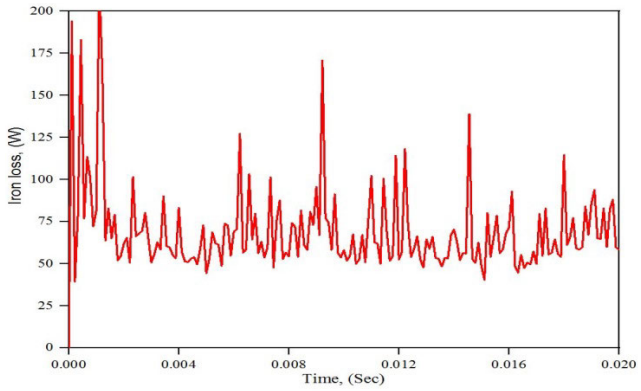

FIGURE 6. Iron losses for the conventional AFPM machine.

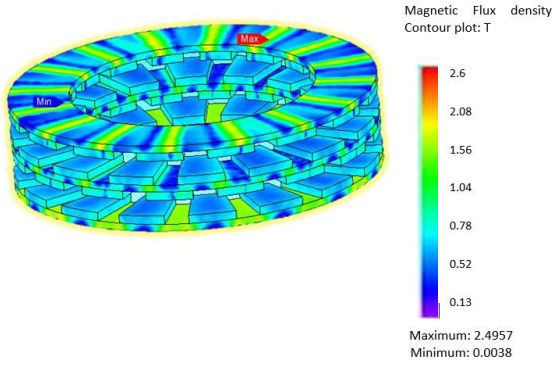

FIGURE 7. Contour plot of the magnetic flux density for the conventional AFPM model.

windings is sinusoidal with slight fluctuations. The RMS for the generated back EMF is 113.826 V. Figure 9 displays the generated output power for this model; the average and RMS power are calculated to be 3,993.86 and 3,996.62 W, respectively. Figure 10 presents the iron losses for the proposed model, with average and RMS values for the generated iron losses of 63.04 and 64.15 W, respectively. In the performed FEA analysis, the eddy current in the rotor core when applying the material to the rotor is considered while calculating

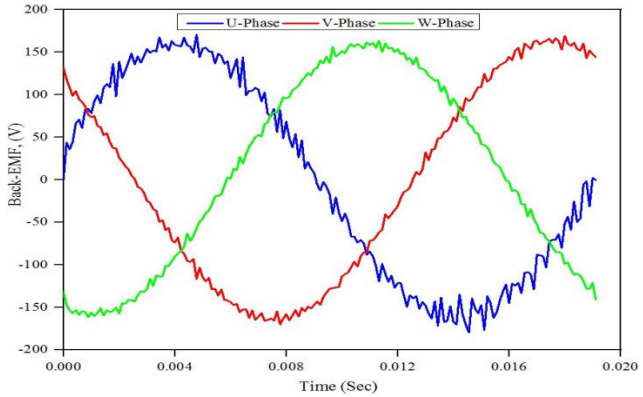

FIGURE 8. Back EMF for the proposed AFPM machine.

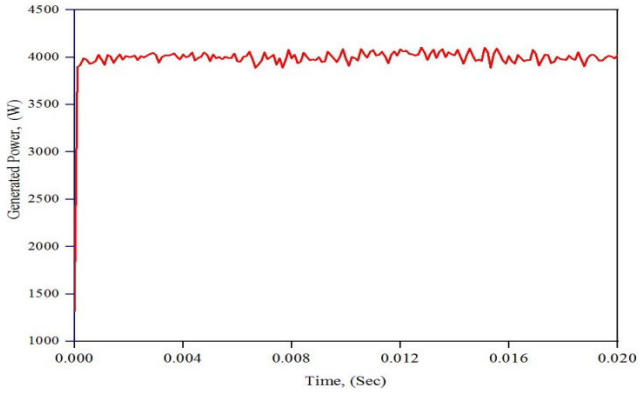

FIGURE 9. Generated output power for the proposed AFPM model.

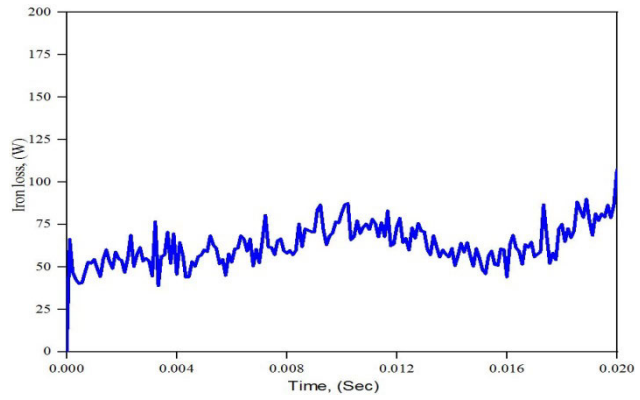

FIGURE 10. Iron losses for the proposed AFPM model.

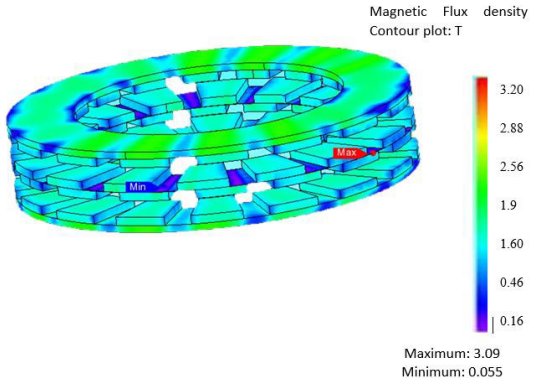

FIGURE 11. Contour plot of the magnetic flux density for the proposed AFPM model.

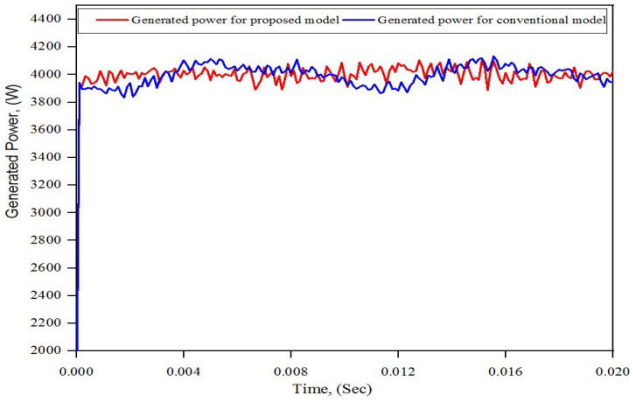

FIGURE 12. Generated output power comparison for the conventional and proposed AFPM machines.

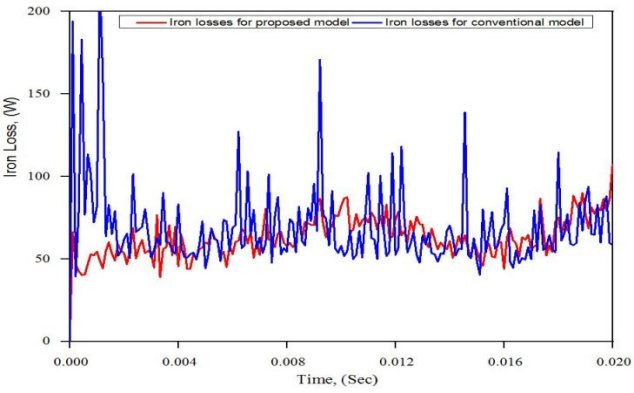

FIGURE 13. Generated iron losses comparison for the conventional and proposed AFPM machines.

the iron losses. Figure 11 shows a contour plot of the magnetic flux density for the proposed AFPM machine.

IV. COMPARATIVE ANALYSIS OF THE CONVENTIONAL AND PROPOSED AFPM MACHINES

Figures 12–13 present a comparison between the conventional and proposed AFPM machines for low-speed applications. Figure 12 shows that the generated output power for the proposed model is higher than that of the conventional model. Figure 13 shows that the iron losses for the conventional model are higher than that of the proposed model, with an overall difference of 10 W; this difference is due to the inner coreless rotor structure of the proposed machine.

Based on this comparative analysis of the conventional and proposed AFPM machines, it can be seen that the proposed topology produces greater output power and reduced losses. Moreover, the contour plot is taken to observe the magnetic

TABLE 4. Comparative analysis of the conventional and proposed topologies.

Parameter	Unit	Conventional model	Proposed model	Comparative results for the proposed model (%)
Back EMF	V_{rms}	108.77	113.83	4.65 ↑
Generated Power	W	3,992.35	3,996.62	0.106 ↑
Iron losses	W	74.14	64.15	13.47 ↓
Magnetic flux density	T	2.45	3.09	26.12 ↑
Efficiency	%	90.0	90.4	0.40 ↑
Axial length	mm	96.8	90.2	6.80↓

TABLE 5. Cost analysis for the conventional and proposed models.

Material	Conventional model		Proposed model	
	Quantity	Cost ($)	Quantity	Cost ($)
Steel for rotor cores	3	10.43	2	6.95
PM for poles	64	137.40	64	137.40
Copper for stator coils	24	58.32	24	58.32
Total	91	206.13	90	202.65

flux density and it shown that proposed model has the higher magnetic flux density.

Table 4 summarizes the comparative analysis of the conventional and proposed models. The performance of the proposed machine is better than that of the conventional AFPM machine, as evaluated using FEA. The proposed topology has a lower weight and a smaller volume than the conventional topology. The cost comparative analysis for the conventional and proposed models is shown in table 5, it is observed that the proposed model is more cost-effective than the conventional model.

A cost analysis for the materials used in permanent magnet machines can be found in [43]. The average cost of steel in US dollars is 1.25 $/kg, while wound copper costs 5.51$/kg, and neodymium–iron–boron (Nd-Fe-B) material, which is used for the magnetic poles, costs 15 $/kg. Labor costs are not considered in the present analysis.

TABLE 6. Weight analysis for the conventional and proposed models.

Material	Conventional model		Proposed model	
	Quantity	Weight (kg)	Quantity	Weight (kg)
Steel for rotor cores	3	8.34	2	5.56
PM for poles	64	9.16	64	9.16
Copper for stator coils	24	10.58	24	10.58
Total	91	28.04	90	25.30

The weight of the conventional and proposed topologies is presented in Table 6. As the tables show, the cost and the weight of the proposed topology are lower than that of the conventional AFPM machine because of the coreless inner rotor. In particular, the cost of the proposed AFPM machine is 1.686% lower than that of the conventional AFPM machine, and the weight is reduced to 9.77%.

V. CONCLUSION

This paper proposes a highly efficient 4-kW AFPM machine for low-speed applications. The performance of the conventional and proposed AFPM machines was compared using FEA to assess the generated output power, back EMF, magnetic flux density, and iron losses. According to the simulation results, the proposed topology offers several advantages, such as higher generated output power, higher efficiency, and reduced iron losses compared to the conventional model. In addition, the proposed AFPM machine has a lower volume and weight.

REFERENCES

[1] X.-M. Li, Z.-X. Yang, Y.-B. Li, W. Chen, and L.-P. Zhang, "Performance analysis of permanent magnet synchronous generators for wind energy conversion system," in *Proc. Int. Conf. Adv. Mechatronic Syst. (ICAMechS)*, Nov./Dec. 2016, pp. 544–549.

[2] X. Yang, D. Patterson, and J. Hudgins, "Permanent magnet generator design and control for large wind turbines," in *Proc. IEEE Power Electron. Mach. Wind Appl. (PEMWA)*, Jul. 2012, pp. 1–5.

[3] M.-J. Kim, B.-K. Kim, J.-W. Moon, Y.-H. Cho, D.-H. Hwang, and D.-S. Kang, "A method for diagnosis of induction machine fed by PWM vector control," *Int. J. Appl. Electromagn. Mech.*, vol. 28, nos. 1–2, pp. 275–281, Sep. 2008.

[4] C.-Y. Hsiao, S.-N. Yeh, and J.-C. Hwang, "Design of high performance permanent-magnet synchronous wind generators," *Energies*, vol. 7, no. 11, pp. 7105–7124, Nov. 2014.

[5] M. Aydin, S. Huang, and T. A. Lipo, "Axial flux permanent magnet disc machines: A review," in *Proc. Conf. Rec. SPEEDAM*, May 2004, pp. 61–71.

[6] J.-H. Choi, Y.-D. Chun, P.-W. Han, M.-J. Kim, D.-H. Koo, J. Lee, and J.-S. Chun, "Design of high power permanent magnet motor with segment rectangular copper wire and closed slot opening on electric vehicles," *IEEE Trans. Magn.*, vol. 46, no. 9, pp. 3701–3704, Sep. 2010.

[7] Z. Zhang, A. Matveev, R. Nilssen, and A. Nysveen, "Ironless permanent-magnet generators for offshore wind turbines," *IEEE Trans. Ind. Appl.*, vol. 50, no. 3, pp. 1835–1846, May 2014.

[8] B. Sheikh-Ghalavand, S. Vaez-Zadeh, and A. H. Isfahani, "An improved magnetic equivalent circuit model for iron-core linear permanent-magnet synchronous motors," *IEEE Trans. Magn.*, vol. 46, no. 1, pp. 112–120, Jan. 2010.

[9] S. A. Kim, J. Li, D.-W. Choi, and Y.-H. Cho, "Design and analysis of axial flux permanent magnet generator for direct-driven wind turbines," *Int. J. Power Syst.*, vol. 2, pp. 1–6, Jan. 2017.

[10] A. Mahmoudi, N. A. Rahim, and H. W. Ping, "Axial-flux permanent-magnet motor design for electric vehicle direct drive using sizing equation and finite element analysis," *Prog. Electromagn. Res.*, vol. 122, pp. 467–496, Jun. 2011.

[11] P. J. Randewijk and M. J. Kamper, "Analytical analysis of a radial flux air-cored permanent magnet machine with a double-sided rotor and non-overlapping double-layer windings," in *Proc. 20th ICEM*, Sep. 2012, pp. 1178–1184.

[12] X. Sun, Y. Shen, S. Wang, G. Lei, Z. Yang, and S. Han, "Core losses analysis of a novel 16/10 segmented rotor switched reluctance BSG motor for HEVs using nonlinear lumped parameter equivalent circuit model," *IEEE/ASME Trans. Mechatronics*, vol. 23, no. 2, pp. 747–757, Apr. 2018.

[13] X. Sun, K. Diao, G. Lei, Y. Guo, and J. Zhu, "Study on segmented-rotor switched reluctance motors with different rotor pole numbers for BSG system of hybrid electric vehicles," *IEEE Trans. Veh. Technol.*, vol. 68, no. 6, pp. 5537–5547, Jun. 2019.

[14] D.-W. Chung and Y.-M. You, "Design and performance analysis of coreless axial-flux permanent-magnet generator for small wind turbines," *J. Magn.*, vol. 19, no. 3, pp. 273–281, 2014.

[15] X. Sun, C. Hu, G. Lei, Y. Guo, and J. Zhu, "State feedback control for a PM hub motor based on grey wolf optimization algorithm," *IEEE Trans. Power Electron.*, vol. 35, no. 1, pp. 1136–1146, Jan. 2020.

[16] Y. Pei, Q. Wang, Y. Bi, and F. Chai, "A novel structure of axial flux permanent magnet synchronous machine with high torque density for electrical vehicle applications," in *Proc. 43rd Annu. Conf. IEEE Ind. Electron. Soc. (IECON)*, Oct./Nov. 2017, pp. 1717–1722.
[17] Z. Shi, X. Sun, Y. Cai, Z. Yang, G. Lei, Y. Guo, and J. Zhu, "Torque analysis and dynamic performance improvement of a PMSM for EVs by skew angle optimization," *IEEE Trans. Appl. Supercond.*, vol. 29, no. 2, pp. 1–5, Mar. 2019.
[18] A. Daghigh, H. Javadi, and H. Torkaman, "Optimal design of coreless axial flux permanent magnet synchronous generator with reduced cost considering improved pm leakage flux model," *Elect. Power Compon. Syst.*, vol. 45, no. 3, pp. 264–278, 2017.
[19] R. J. Wang, M. J. Kamper, K. Van der Westhuizen, and J. F. Gieras, "Optimal design of a coreless stator axial flux permanent-magnet generator," *IEEE Trans. Magn.*, vol. 41, no. 1, pp. 55–64, Jan. 2005.
[20] T. D. Nguyen, K.-J. Tseng, S. Zhang, and H. T. Nguyen, "A novel axial flux permanent-magnet machine for flywheel energy storage system: Design and analysis," *IEEE Trans. Ind. Electron.*, vol. 58, no. 9, pp. 3784–3794, Sep. 2011.
[21] X. Sun, C. Hu, J. Zhu, S. Wang, W. Zhou, Z. Yang, G. Lei, K. Li, B. Zhu, and Y. Guo, "MPTC for PMSMs of EVs with multi-motor driven system considering optimal energy allocation," *IEEE Trans. Magn.*, vol. 55, no. 7, Jul. 2019, Art. no. 8104306.
[22] X. Sun, B. Su, S. Wang, Z. Yang, G. Lei, J. Zhu, and Y. Guo, "Performance analysis of suspension force and torque in an IBPMSM with V-shaped PMs for flywheel batteries," *IEEE Trans. Magn.*, vol. 54, no. 11, Nov. 2018, Art. no. 8105504.
[23] Q. A. S. Syed, Y.-M. You, and B.-I. Kwon, "Design and comparative analysis of single and multi-stack axial flux permanent magnet synchronous generator," *Int. J. Appl. Electromagn. Mech.*, vol. 39, nos. 1–4, pp. 865–872, 2012.
[24] J. Zhang, M. Cheng, and Z. Chen, "Optimal design of stator interior permanent magnet machine with minimized cogging torque for wind power application," *Energy Convers. Manage.*, vol. 49, pp. 2100–2105, Aug. 2008.
[25] M. M. Ashraf and T. N. Malik, "Design of a three-phase multistage axial flux permanent magnet generator for wind turbine applications," *Turkish J. Elect. Eng. Comput. Sci.*, vol. 25, no. 1, pp. 520–538, 2017.
[26] X.-M. Li, Z.-X. Yang, and D.-L. Song, "A novel outer rotor axial primary magnetic circuit permanent magnet generator," in *Proc. Int. Conf. Adv. Mechatronic Syst.*, Aug. 2015, pp. 20–23.
[27] B. Zhang and M. Doppelbauer, "Iron losses calculation of an axial flux machine based on three-dimensional FEA results corresponding to one-sixth electrical period," *IEEE Trans. Energy Convers.*, vol. 32, no. 3, pp. 1023–1030, Sep. 2017.
[28] M. J. Kamper, J. H. J. Potgieter, J. A. Stegmann, and P. Bouwer, "Comparison of air-cored and iron-cored non-overlap winding radial flux permanent magnet direct drive wind generators," in *Proc. IEEE Energy Convers. Congr. Expo.*, Sep. 2011, pp. 1620–1627.
[29] J. P. Lim, J. S. Rho, K. P. Yi, J. M. Seo, and H. K. Jung, "Characteristic analysis of a traveling wave ultrasonic motor using an ellipsoidal static contact model," *Smart Mater. Struct.*, vol. 18, no. 11, Sep. 2009, Art. no. 115024.
[30] J. S. Rho, C. H. Lee, T.-K. Chung, C.-H. Im, and H. K. Jung, "Analysis of a nanopositioning actuator using numerical and analytic methods," *Smart Mater. Struct.*, vol. 17, no. 2, Feb. 2008, Art. no. 025025.
[31] H. Tiegna, Y. Amara, and G. Barakat, "Overview of analytical models of permanent magnet electrical machines for analysis and design purposes," *Math. Comput. Simul.*, vol. 90, pp. 162–177, Apr. 2013.
[32] D. N. Mbidi, "Design and evaluation of a 300 kw double stage axial-flux permanent magnet generator," presented at the Ind. Appl. Conf., Rome, Italy, Dec. 2001.
[33] S. S. Soe and Y. A. Oo, "Design of the coreless axial-flux double-sided permanent magnet synchronous generator for wind power system," *Int. J. Sci. Eng. Technol. Res.*, vol. 3, no. 10, pp. 2047–2051, May 2014.
[34] A. Aghili, M. R. Besmi, and M. A. Ghadamyari, "A novel structure for axial flux permanent magnet machines with internal stator," in *Proc. 3rd Power Electron. Drive Syst. Technol.*, Tehran, Iran, Feb. 2012, pp. 68–73.
[35] A. Mahmoudi, N. A. Rahim, and W. P. Hew, "Axial-flux permanent-magnet machine modeling, design, simulation, and analysis," *Sci. Res. Essays*, vol. 6, no. 12, pp. 2525–2549, Jun. 2011.
[36] M. R. Minaz and M. Çelebi, "Design and analysis of a new axial flux coreless PMSG with three rotors and double stators," *Results Phys.*, vol. 7, pp. 183–188, Jan. 2017.
[37] A. Daghigh, H. Javadi, and H. Torkaman, "Design optimization of direct-coupled ironless axial flux permanent magnet synchronous wind generator with low cost and high annual energy yield," *IEEE Trans. Magn.*, vol. 52, no. 9, Sep. 2016, Art. no. 7403611.
[38] I. Stamenkovic, N. Milivojevic, N. Schofield, M. Krishnamurthy, and A. Emadi, "Design, analysis, and optimization of ironless stator permanent magnet machines," *IEEE Trans. Power Electron.*, vol. 28, no. 5, pp. 2527–2538, May 2013.
[39] A. Mahmoudi, S. Kahourzade, N. A. Rahim, H. W. Ping, and M. N. Uddin, "Design and prototyping of an optimised axial-flux permanent-magnet synchronous machine," *IET Electr. Power Appl.*, vol. 7, no. 5, pp. 338–349, May 2013.
[40] M. Aydin, S. Huang, and T. A. Lipo, "A new axial flux surface mounted permanent magnet machine capable of field control," in *Proc. 37th IAS Annu. Meeting Conf. Rec. IEEE Ind. Appl. Conf.*, Oct. 2002, pp. 1250–1257.
[41] H.-K. Yeo and J.-S. Ro, "Novel analytical method for overhang effects in surface-mounted permanent-magnet machines," *IEEE Access*, vol. 7, pp. 148453–148461, 2019.
[42] D.-K. Lim and J.-S. Ro, "Analysis and design of a delta-type interior permanent magnet synchronous generator by using an analytic method," *IEEE Access*, vol. 7, pp. 85139–85145, 2019.
[43] J. F. Gieras, R.-J. Wang, and M. J. Kamper, *Axial Flux Permanent Magnet Brushless Machines*. Dordrecht, The Netherlands: Springer, 2008.

SAHIB KHAN received the B.E. degree in electrical engineering and the M.E. degree in renewable energy systems from Sukkur IBA University, Sukkur, Pakistan. His research interest includes the designing and analysis of electrical machines.

SYED SABIR HUSSAIN BUKHARI (M'16) was born in Khairpur, Sindh, Pakistan, in 1986. He received the B.E. degree in electrical engineering from the Mehran University of Engineering and Technology, Jamshoro, Pakistan, in 2009, and the Ph.D. degree from the Department of Electronic Systems Engineering, Hanyang University, South Korea, in 2017. He joined Sukkur IBA University, in December 2016, as an Assistant Professor. He is currently a Research Professor with Chung-Ang University, Seoul, South Korea, under Korean Research Fellowship (KRF) Program. His main research interests include electric machine design, power quality, and drive controls.

JONG-SUK RO received the B.S. degree in mechanical engineering from Hanyang University, Seoul, South Korea, in 2001, and the Ph.D. degree in electrical engineering from Seoul National University (SNU), Seoul, in 2008.

He conducted research at the Research and Development Center, Samsung Electronics, as a Senior Engineer, from 2008 to 2012. From 2012 to 2013, he was with the Brain Korea 21 Information Technology of SNU, as a Postdoctoral Fellow. He conducted research at the Electrical Energy Conversion System Research Division, Korea Electrical Engineering and Science Research Institute, as a Researcher, in 2013. From 2013 to 2016, he worked with the Brain Korea 21 Plus, SNU, as a BK Assistant Professor. In 2014, he was with the University of Bath, Bath, U.K. He is currently an Associate Professor with the School of Electrical and Electronics Engineering, Chung-Ang University, Seoul. His research interests include the analysis and optimal design of next-generation electrical machines using smart materials, such as electromagnet, piezoelectric, and magnetic shape memory alloy.